Available online at www.sciencedirect.com
ScienceDirect
Acta Materialia 58 (2010) 4516–4526
Acta MATERIALIA
www.elsevier.com/locate/actamat

Filler-reduced phonon conductivity of thermoelectric skutterudites: Ab initio calculations and molecular dynamics simulations

Baoling Huang, Massoud Kaviany *

Department of Mechanical Engineering, University of Michigan, Ann Arbor, MI 48109, USA

Received 6 December 2009; received in revised form 29 April 2010; accepted 2 May 2010
Available online 25 May 2010

Abstract

The phonon conductivities of $CoSb_3$ and its Ba-filled structure $Ba_x(CoSb_3)_4$ are investigated using first-principle calculations and molecular dynamics (MD) simulations, along with the Green–Kubo theory. The effects of fillers on the reduction of the phonon conductivity of filled skutterudites are then explored. It is found that the coupling between filler and host is strong, with minor anharmonicity. The phonon density of states and its dispersion are significantly influenced by filler-induced softening of the host bonds (especially the short Sb–Sb bonds). Lattice dynamics and MD simulations show that, without a change in the host interatomic potentials, the filler–host bonding alone cannot lead to significant alteration of acoustic phonons or lowering of phonon conductivity. The observed smaller phonon conductivity of partially filled skutterudites is explained by treating it as a solid solution of the empty and fully filled structures.
© 2010 Acta Materialia Inc. Published by Elsevier Ltd. All rights reserved.

Keywords: Semiconductor compounds; Simulation; Thermal conductivity; Molecular dynamics

1. Introduction

Binary skutterudites are structures with the general formula MX_3 (*Im*3), where M is one of the group 9 transition metals (Co, Rh, or Ir), and X is a pnictogen. Skutterudites are characterized by a complex cubic crystalline structure containing large cages and four-membered planar rings of X (shown in Fig. 1) [1]. These large cages can be filled with other undersized atoms, e.g. rare-earth (Re) atoms. It has been observed that filling the cages leads to a dramatic decrease in the phonon conductivity [2,3]. Due to their good electronic properties (high Seebeck coefficient and high electrical conductivity), this reduction in phonon conductivity makes the filled skutterudites promising for thermoelectric applications.

The significant decrease in phonon conductivity in filled skutterudites has been explained through the strong anharmonic rattling motion of the loosely bonded filling atoms in the skutterudite cages [2]. Large atomic displacement parameters of the filler in the filled skutterudites with significantly reduced phonon conductivity has been observed [4]. Inelastic neutron scattering measurements on $LaFe_4Co_{12}$ also show a well-defined peak (56 cm^{-1} at the low-frequency regime of phonon density of states [5]). Perhaps the most important evidence of rattling comes from the investigations of low-temperature specific heat measurements [5], which suggest the presence of Einstein oscillators.

However, this "rattling" theory is not unarguable yet. It has been observed that a relatively small concentration of a filler can cause a relatively large decrease in the phonon conductivity of skutterudites [6,2,3,7]. In addition, the largest decrease in phonon conductivity is achieved for the partially filled skutterudites rather than the fully filled structures [2,3]. If this reduction in phonon conductivity is due to the scattering by "rattlers", then we can expect the phonon conductivity to decrease monotonically with increasing filler concentration. However, observations show that there exists an optimal filling fraction in reducing the phonon conductivity [2,3,7]. Moreover, the room-temperature phonon conductivity of some partially filled

* Corresponding author.
E-mail address: kaviany@umich.edu (M. Kaviany).

1359-6454/$36.00 © 2010 Acta Materialia Inc. Published by Elsevier Ltd. All rights reserved.
doi:10.1016/j.actamat.2010.05.002

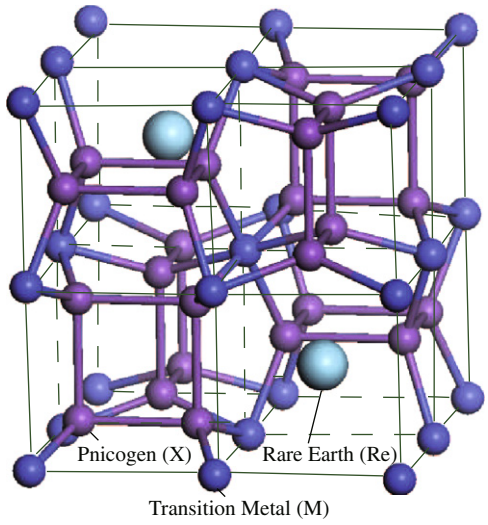

Fig. 1. Cubic structure of the skutterudites. Two rare-earth fillers in adjacent cages are also shown.

skutterudites [7], e.g. $Ce_yFe_xCo_{4-x}Sb_{12}$, is almost independent of the filling fraction when the filling fraction is larger than 0.2. Nolas et al. [2] argued that a point-defect-type phonon scattering effect, due to the partial, random distribution of fillers in the voids, as well as the "rattling" effect of the filler ions, results in the scattering of a larger spectrum of phonons than in the case of full filling.

To clarify the mechanisms in the reduction of phonon conductivity in filled skutterudites, investigation into the phonon transport at the atomic level is required. The present work reports the lattice dynamics calculations and direct molecular dynamic (MD) simulations for the thermal conductivities of $CoSb_3$ and its filled structure, $Ba_x(CoSb_3)_4$, on the basis of quantum mechanics, which provides important information for the filler–host interaction and interphonon scattering. First, the vibration spectrum and dispersion of the empty and filled $CoSb_3$ structure are calculated and compared. Then the force fields for this two structures are developed using ab initio calculations. Together with the Green–Kubo (G–K) method, the MD simulations are used to directly predict the thermal conductivity of the two structures. Thereafter, the role of filler in determining the phonon transport is discussed and modelled.

2. Calculation details

Ab initio calculations were performed for the empty $CoSb_3$ and its filled structures using the ABINIT package [8] within the density-functional theory (DFT) framework. A planewave basis and the general gradient approximation (GGA), parameterized by Perdew et al. [9] to the exchange-correlation potential, were adopted in the calculations. The normal-conserving pseudopotentials with the Troullier–Martins scheme were used to replace the all-electron core potentials. No significant deviation between the reported results with and without spin-orbit coupling included was found, so it is neglected in the following calculations.

Both the lattice constants and atomic positions of $CoSb_3$ and the filled structures were relaxed until the forces on the atoms were smaller than 2.6×10^{-3} eV/Å. By changing the κ-points and the kinetic energy cutoff involved in the calculations, a $2 \times 2 \times 2$ grid of special κ-points and a kinetic energy cutoff of 35 Hartree were found to be sufficient to obtain well-converged energy and phonon frequency results.

For convenience, most of the calculations in this work focused on the empty $CoSb_3$ and Ba-filled structure ($Ba_x(CoSb_3)_4$). However, some calculations for other fillers (e.g. Ce and Yb) were also carried out to show the transferability of the results. In the calculations, we used the same parameters as used for Ba.

3. Empty and filled structure

3.1. Filling effects on lattice

Here the empty $CoSb_3$ and fully Ba-filled structure $Ba(CoSb_3)_4$ are considered to investigate the effects of filling on the lattice parameters. Although the formation enthalpy for filling atoms into $CoSb_3$ structure is negative, so far no fully Ba-filled $CoSb_3$ cage has been made (due to the existence of secondary phase [10]). However, since the bonds in the structures are of strong covalent characters

Table 1
Comparison among the structure parameters of $CoSb_3$ and $Re_x(CoSb_3)_4$ (Re = Ba, Ce, Yb) from the ab initio calculations and some theoretical and experimental results in the literature [13,14,12,15].

Parameters	a (Å)	u	v	Co–Sb (Å)	Sb–Sb (Å)
$CoSb_3$	9.14 (GGA) [13]	0.3332 (GGA) [13]	0.1594 (GGA) [13]		
	8.94 (LDA) [13]	0.3328 (LDA) [13]	0.1599 (LDA) [13]		
	9.04 (Exp.) [12]	0.3354 (Exp.) [12]	0.1579 (Exp.) [12]	2.53 (Exp.)[a]	2.90/2.98 (Exp.)[a]
	9.14 (GGA, this work)	0.3346 (GGA, this work)	0.1585 (GGA, this work)	2.55 (GGA, this work)	2.89/3.03 (GGA, this work)
$Ba(CoSb_3)_8$	9.12 (LDA) [15]	0.3334/0.3360 (LDA) [15]	0.1587/0.1605 (LDA)	2.52/2.53 (LDA)[a]	2.93/3.03 (LDA)[a]
$Ba(CoSb_3)_4$	9.27 (GGA, this work)	0.3386 (GGA, this work)	0.1619 (GGA, this work)	2.59 (GGA, this work)	2.99/3.00 (GGA, this work)
$Ce(CoSb_3)_4$	9.26 (GGA, this work)	0.3351 (GGA, this work)	0.1613 (GGA, this work)	2.58 (GGA, this work)	2.99/3.04 (GGA, this work)
$Yb(CoSb_3)_4$	9.26 (GGA, this work)	0.3333 (GGA, this work)	0.1592 (GGA, this work)	2.58 (GGA, this work)	2.95/3.09 (GGA, this work)

Note that for this work $x = 1$, and for Ref. [15] $x = 0.5$. [a] The values are calculated from the published lattice parameters [15,12].

[11], this fully filled treatment can still provide useful information about the filler–host interactions. The calculated structure parameters and their comparison with some other calculations are shown in Table 1. The lattice constant of the relaxed $CoSb_3$ is $a = 9.14$ Å, which is slightly larger than the experimental value [12] $a = 9.04$ Å. However, it is the same as the DFT (GGA) result predicted by Mahan [13]. The internal parameters u and v for the relaxed $CoSb_3$ structure are in good agreement with both the experimental and DFT results in the literature [13,14,12]. For $Ba(CoSb_3)_4$, the comparison with the LDA calculations for half-filled $Ba(CoSb_3)_8$ performed by Kajitani et al. [15] shows a reasonable agreement. Table 1 shows that the addition of Ba filler will slightly increase the lattice constant as well as the internal parameters u and v. This is also apparent in the calculations [15] for the half-filled $Ba(CoSb_3)_8$, which show a larger lattice constant and two groups of Sb sites. The most significant change is the bond length for the short Sb–Sb bond, which increases from 2.888 to 2.993 Å. Thus the intra-rectangular pnicogen ring becomes closer to a square in the fully filled structure. Similar results are also found for other fully filled $Re(CoSb_3)_4$ (Re = Ce, Yb) structures (shown in Table 1).

3.2. Filler–host interaction

The GGA calculations using the ABINIT package[8] were also adopted to investigate the interactions between the filler and the host. Fig. 2a shows the variation of calculated total energy of $BaCo_8Sb_{24}$ with respect to the absolute displacements from the center of the cage along the [1 0 0], [1 1 0] and [1 1 1] directions. Apparently, the three curves overlap quite well, indicating the energy surface for the filler–host interactions is isotropic. At the same time, Fig. 2b shows the dependence of the calculated lattice energy of $ReCo_8Sb_{24}$ on the square of the displacement d from the center along the [1 0 0] direction, for various fillers (Re = Ba, Ce and Yb). The dashed lines show the slope of the calculated energy curve at the cage center, representing the prediction of the harmonic model with a force constant at $d = 0$. This harmonic approximation predicts the calculated potential energy curve fairly well. Some anharmonic deviation are marginally evident at large displacements, but even at the large displacements (around 0.5 Å) and for all the fillers the deviation in potential energy is within 5% and the force constants differ from the values at the cage center only by less than 10%. The vibration frequency shifts due to anharmonicity is expected to be less than 5%. Therefore, the anharmonicity of the filler–host interaction is considered to be rather weak. Similar behavior is also found in $La(Ce)Fe_4Sb_{12}$ [16,17] and $TlFeCo_3Sb_{12}$ [11]. Fig. 2b also shows that the order of the bare force constant for the fillers is Ba > Ce > Yb, that is, the heavier the filler, the smaller bare force constant and in turn the lower bare vibration frequency. From Fig. 2b, we can obtain the bare vibration frequencies for Ba, Ce and Yb, which are 3.31, 2.23 and 1.80 THz, respectively. The bare frequencies for

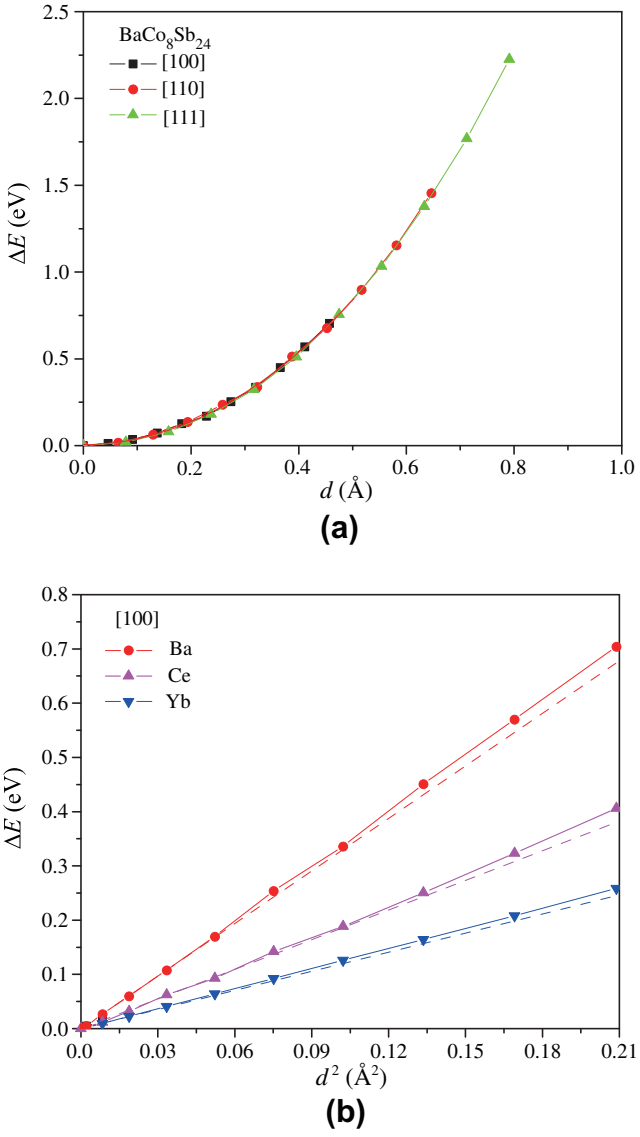

Fig. 2. (a) Variations of calculated total energy of $BaCo_8Sb_{24}$ with respect to displacements from the center of the cage along the [1 0 0], [1 1 0] and [1 1 1] directions. (b) Variations of calculated total energy of $ReCo_8Sb_{24}$ (Re = Ba, Ce, Yb) with respect to displacement from the center of the cage along [1 0 0] directions. The dashed lines show the slopes of those LDA/GGA energy curves at $d^2 = 0$, representing the prediction from a harmonic model.

Ce obtained here are slightly higher than those [16] reported for Ce (2.04 THz) in $La(Ce)Fe_4Sb_{12}$. Since interaction between the filler and the host is of strong covalent characters [11], we assumed the filler interacts only with the nearest Sb and Co neighbors and then fitted the interatomic force constants with the scanned filler–host energy surface. The results are shown in Table 2. The fitted force

Table 2
Fitted force constants for the interaction between the filler Re (Re = Ba, Ce, and Yb) and host atoms in $CoSb_3$.

Force constants	Ba	Ce	Yb
Γ_{Re-Sb} (eV/Å^2)	1.70	0.96	0.63
Γ_{Re-Co} (eV/Å^2)	0.008	0.033	0.0027

constants show that all the fillers have a strong coupling with the nearest Sb atoms, but the coupling with Co atoms is very weak due to the longer separation. This is consistent with the calculations about the Sb cage deformation reported in the literature [18]. This is also confirmed by the response–function theory calculations shown below. In the following calculations, Ba was chosen as the filler for the investigation as a high filling fraction was achieved experimentally with this filler [19].

The interatomic force constants Γ_{i-j} can be directly determined using the response–function theory (RFT) [20], which is a density-functional linear response approach to dynamical matrix calculations. By applying perturbations based on the structure symmetry and calculating the corresponding first- and second-order gradients of bond energy, the dynamical matrix can be constructed and the real space interatomic force constant can be in turn extracted [20]. Those force constants were projected on the local coordinates to be decomposed into the longitudinal and transversal force constants. The resulting longitudinal force constants Γ_L are expected to correspond to the two-body stretching force constant, and the transversal force constants Γ_T are believed to result from the many-body interactions.

Fig. 3 shows the comparison of the calculated longitudinal force constants of $CoSb_3$ and $Ba(CoSb_3)_4$ structure. The force constant values that change significantly after the Ba insertion into the cage vacancy are shown in a box. Fig. 3 shows that, except for Co–Sb bonds, the force constants of other bonds are more or less changed by the Ba filler. The most important change is Γ_L of the short Sb–Sb bond, which decreases around 50% and becomes close to that of the long Sb–Sb bond. Also, Γ_L of Co–Co almost vanishes in the filled structure. Γ_L of the long Sb–Sb bond and the Sb–Sb inter-rectangle bond also decrease, by 10 and 20%, respectively. This softening seems to result from the antibonding states caused by the filler. Similar results were found for fully Ce-filled $CoSb_3$ structure. The calculated Γ_L of the Sb–Ba interaction is 1.66 eV/Å^2, in good agreement with the 1.7 eV/Å^2 (shown in Table 2) obtained by fitting the energy surface. This bond softening is also reported in the literature on skutterudites filled with other atoms [21,22].

4. Lattice dynamics

To clarify the effects of the fillers on the lattice vibrations of skutterudite structure, the phonon density of states (DOS) and dispersions for different filled and unfilled skutterudite structures have been intensively investigated [14,11,18,23]. Here we present the normalized total DOS and dispersion curves of the unfilled $CoSb_3$ and the filled $Ba(CoSb_3)_4$ calculated using RFT and lattice dynamics. Fig. 4a and b shows the calculated phonon DOS of $CoSb_3$ and $Ba(CoSb_3)_4$, respectively. The calculated DOS for $CoSb_3$ is in good agreement with the other calculations in the literature [14,11]. In Fig. 4a, the high-frequency spectrum is mainly due to the vibration of Co and the low-frequency spectrum is mainly due to the vibration of Sb [11]. This is believed to be due to their very different masses. At the same time, Fig. 4 shows that the existence of the filler, Ba atoms, significantly affects the overall total vibration spectrum. This is believed to be due to the strong coupling between the filler and the host.

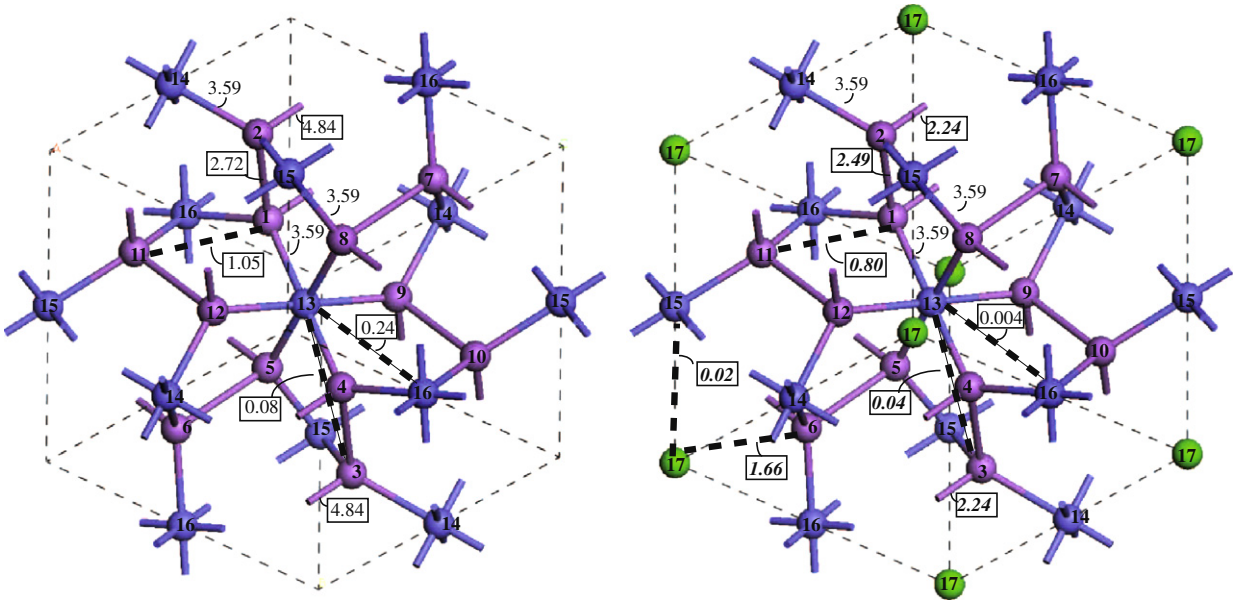

$a = 9.14$ Å, $u = 0.1585$, $v = 0.3346$ (a)

$a = 9.27$ Å, $u = 0.1619$, $v = 0.3386$ (b)

Fig. 3. Comparisons between the longitudinal force constants Γ_{i-j} of $CoSb_3$ and $Ba(CoSb_3)_4$, obtained from the ab initio calculations and from RFT. Atoms 1–12 are Sb atoms, 13–16 are Co atoms and 17 is Ba atom. The values that changes significantly due to the addition of filler are shown in box.

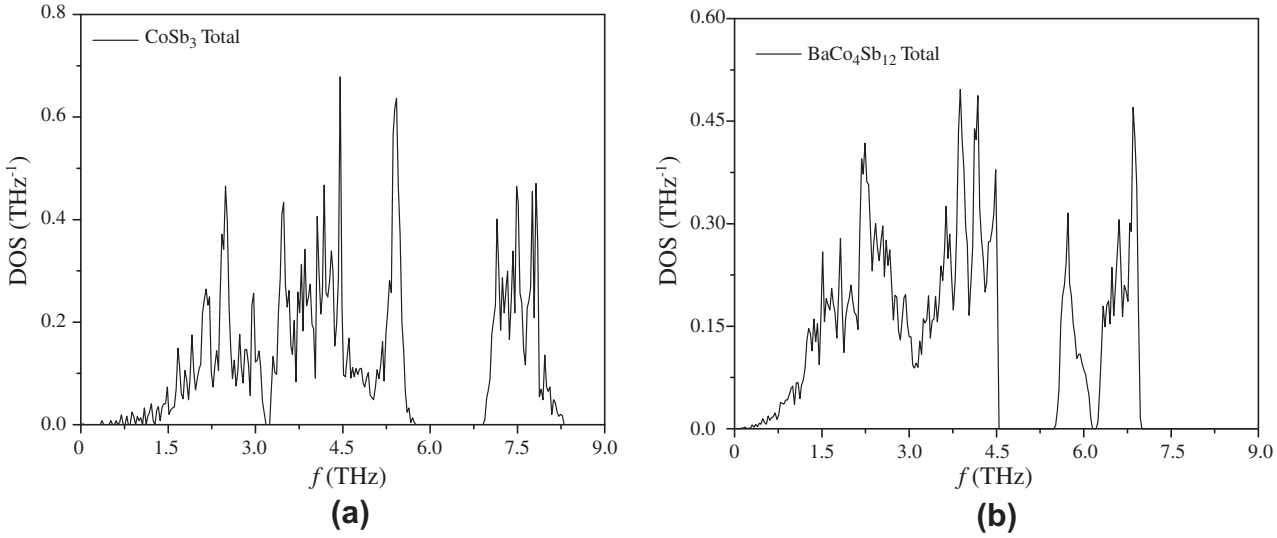

Fig. 4. (a) Normalized phonon DOS of $CoSb_3$. (b) Normalized phonon DOS of $Ba(CoSb_3)_4$.

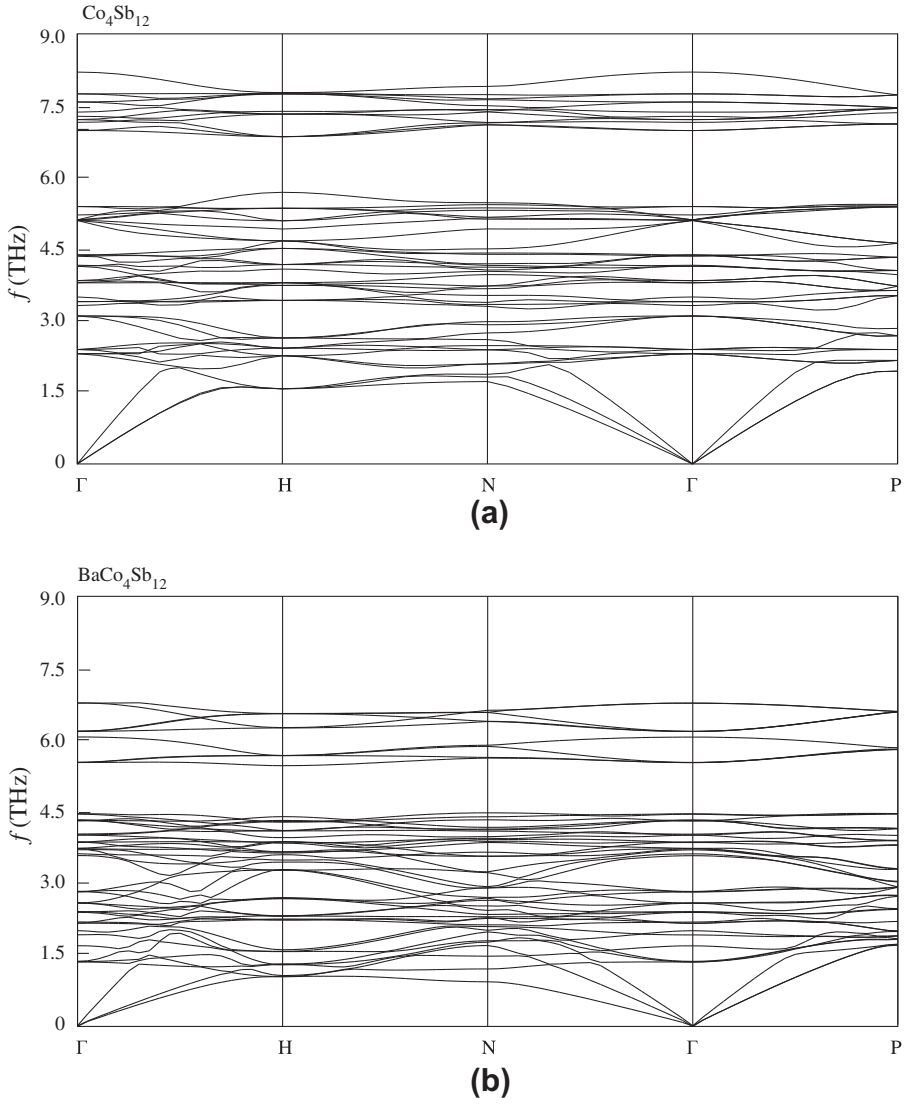

Fig. 5. Phonon dispersion calculated by RFT for (a) Co_4Sb_{12} and (b) $Ba(CoSb_3)_4$.

Phonon dispersion may provide more information on the effects of the filler in $CoSb_3$ structure. Fig. 5 shows the phonon dispersion of (a) $CoSb_3$ and (b) $Ba(CoSb_3)_4$. The dispersion curves for $CoSb_3$ seem to be significantly changed by Ba atoms. First, the acoustic branches become flatter and their cutoff frequency is reduced from around 1.5 to 1.0 THz, which means the group velocity of acoustic branches is reduced by around 30%. Secondly, the optical branches are squeezed, i.e. both the vibration frequency and group velocity are reduced. Furthermore, there are more dispersion curves near 2 THz. These changes in the dispersion, however, seem to be due not to the disturbance of the Ba vibration, as proposed in the "rattling" model, but to the weakened bond force constant, caused by the presence of the Ba atom. This is more clear by comparing the dispersion curves from ab initio calculations (Fig. 5a and b) with those calculated using classic force fields and lattice dynamics (as shown in Fig. 6). In Fig. 6a, the potential model C proposed by Feldman and Singh [14] was adopted for the $CoSb_3$ host; in Fig. 6b, the Feldman–Singh model was used together with the filler–host interaction fitted with the scanned energy surface (as mentioned in Section 3). Fig. 6a shows that the dispersion for the empty $CoSb_3$ structure calculated from Feldman–Singh model is in good agreement with the results from RFT. When the Ba atom is inserted into the cage, as shown in Fig. 6b, the overall change in the dispersion is minor if the force field for the host remains the same. The acoustic branch below 1.5 THz is almost untouched and the optical phonon spectrum between 1.5 and 6 THz actually expands, which is in contrast with the result shown in Fig. 5b. Comparing the dispersions for the empty and filled structure, phonon transport is more likely to be suppressed in the filled structure with a dispersion shown in Fig. 5b.

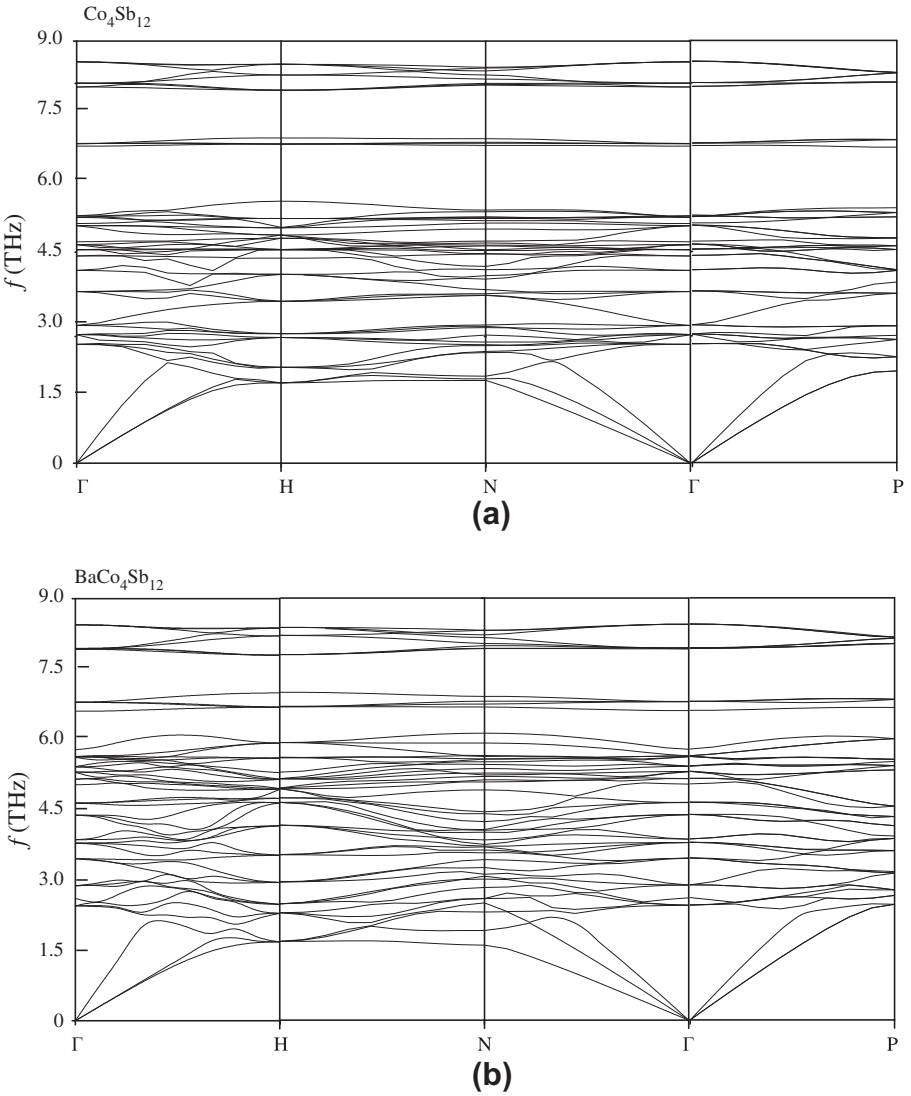

Fig. 6. Phonon dispersion calculated by the classical force field for (a) Co_4Sb_{12} and (b) $Ba(CoSb_3)_4$. The model C of Ref. [14] was adopted for the $CoSb_3$ host, and the filler–host interaction was fitted with the scanned energy surface.

5. Thermal conductivities of empty and filled structures

5.1. MD simulation procedure and G–K autocorrelation

The direct calculations of the phonon conductivity may provide important information for the role of the filler. The phonon thermal conductivity $\boldsymbol{K}_p$ of unfilled and filled $CoSb_3$ can be determined using MD simulations together with the G–K approach. In this approach, the thermal conductivity $\boldsymbol{K}_p$ tensor can be obtained from the decay of the heat current autocorrelation function (HCACF) as [24–26]

$$\boldsymbol{K}_p = \frac{1}{k_B V T^2}\int_0^\infty \langle \dot{\boldsymbol{w}}(t)\dot{\boldsymbol{w}}(0)\rangle, \tag{1}$$

where k_B is the Boltzmann constant, V is the volume of the simulation system, T is the system temperature and $\langle \dot{\boldsymbol{w}}(t)\cdot\dot{\boldsymbol{w}}(0)\rangle$ is the HCACF. A slow-decaying HCACF indicates a long phonon relaxation time. The heat current $\dot{w}$ is defined as

$$\dot{w} = \frac{\mathrm{d}}{\mathrm{d}t}\sum_{i=1}^{N} r_i E_i, \tag{2}$$

where $\boldsymbol{r}$ and E are the position vector and the energy of a particle (atom) (excluding the site energy), respectively.

Because of their cubic structures, the phonon thermal conductivities of $CoSb_3$ and the filled structure ($ReCo_8Sb_{24}$) are isotropic. Due to the limit computation resource, to minimize the computation time, the MD simulations were mainly performed with a system consisting of $12\times3\times3$ cubic unit cells ($117\times27\times27$ Å^3). We assumed the phonon transport in the x direction would not be significantly affected by the small dimensions in the other two directions. This assumption was confirmed by running a simulation using the same force field and a $9\times9\times9$ unit-cell system. The obtained results for the $9\times9\times9$ unit-cell system were found to be very close to the x-direction results for the $12\times3\times3$ unit-cell system. The simulations with even larger systems, e.g. a $15\times4\times4$ system, produced very similar results, indicating that the size effects were minor for a $12\times3\times3$ system. All the simulations were performed at 300 K and the time step was chosen as 4 fs. The Verlet leap-frog algorithm was adopted for the calculation, while the Nose–Hoover thermostat and the Berendsen barostat were used to control the system temperature and pressure. The system was first simulated in an NPT (constant number of atoms, pressure and temperature) ensemble for 100–200 ps until it reached a free-standing state at the desired temperature, then it was switched into an NVE ensemble and run for another 100 ps to reach the equilibrium state. Thereafter, 3000 ps raw heat current data were obtained for the calculation of HCACFs. The resultant HCACFs were then directly integrated and the phonon conductivities were set as the average values in the stable regime of the integral.

5.2. Interatomic potentials

The MD calculations require suitable force fields for the empty and filled structures. Lutz and Kliche [27] (LK) fitted a six-parameter central force constant model to the infrared data of $CoSb_3$. Their model accurately predicts the LDA volume dependence of the total energy and most eigen mode frequencies. However, the LK model does not contain bond angle force constants, which may be important due to the significance of covalent bonding in $CoSb_3$ structure. Feldman et al. [22] proposed a harmonic force field which includes the bond-angle distortions by fitting the parameters to the available infrared data and LDA results. They also fitted the cubic anharmonic terms of the interatomic potentials with the LDA results. Their model predicts the zone-center mode frequencies and the anharmonicity in the volume-dependent LDA results quite well. The effects of atomic charges are assumed to be negligible in Feldman's model as well as in the LK model, due to the strong covalent characters of the interatomic bond. Nevertheless, a cubic bond-stretching potential passes through a maximum and might cause some instability in the molecular dynamics for some cases. Therefore, the quadratic anharmonic terms should be involved for a robust MD simulation, which, however, is very challenging to fit accurately. Therefore, for direct MD simulations, we changed the potential forms of Feldman's model while keeping the harmonicity and the third-order anharmonicity, which dominate the phonon transport. Of the many functional forms used to model interatomic interactions, the Morse potential is found to be very useful, especially for covalent bonds. The Morse potential has the following form [24]

$$\varphi = \varphi_\circ\{[1-\exp(-a(r-r_\circ))]^2 - 1\}, \tag{3}$$

where $\varphi_\circ$ is the depth of the potential energy minimum and $r_\circ$ is the equilibrium bond length. We first determined the parameters in the Morse potentials for $CoSb_3$ by fitting their harmonic and cubic anharmonic terms with the force field proposed by Feldman et al. [22]. That force field model includes the nearest-neighbor Co–Sb interaction, the nearest-neighbor Co–Co interaction, the two nearest-neighbor Sb–Sb interactions (both long and short bonds) in the rectangles, the two nearest-neighbor Sb–Sb interactions between rectangles and the two bond-angle distortions associated with the two distinct Co–Sb–Sb angles. As expected, this force field produces the same predictions for the zone-center normal modes and elastic constants as those calculated by Feldman et al. [14]. The fitted potential for the filler–host was used for the filled structure. The above force fields were used in MD to determine how the filler movements affect the thermal conductivity.

However, as mentioned, for a filled skutterudite structure, the filler may significantly affect the interatomic interactions. Therefore, for the direct comparison between the empty structure and the fully filled one, we also need to obtain the potentials for filled $CoSb_3$ structure as well as the empty one on the same platform and using the same approach. Normally, interatomic potentials are developed by fitting the energy surface scanned by the ab initio calculations or the experimental data, which is extremely challenging due to the difficulty in decomposing the different

interactions. With the motivation from the dynamical matrix calculations in Section 4, a new approach based on the response function theory [8,28,29] was also adopted here. First, the interatomic force constants for the optimized structure were calculated. Then, by varying the lattice constant, a series of force constants were obtained. Providing the interatomic bond model, these force constants together with the corresponding bond length were then analyzed to obtain the anharmonic terms. Thereafter, the Morse potentials were fitted with these harmonic and anharmonic terms, and the results are listed in Table 3. This method is valid as long as the atoms considered are not too far away from their equilibrium positions.

5.3. Effects of fillers

Fig. 7 shows the time evolution of the predicted phonon conductivity of $CoSb_3$ at $T = 300$ K, using the modified force field (model C) developed in Ref. [22]. This force field leads to a k_p of 6.3 W m^{-1} K^{-1}. This value is lower than the experimental results (k_p of between 8 and 11 W m^{-1} K^{-1}) [2,30,19]. This lower value might be due to the overestimation of Grüneisen parameter, which is calculated as $\gamma_G = 1.1$ and is higher than the experimental value [30] $\gamma_G = 0.95$. By adding the Ba–Sb fitted potential while keeping the force field for the host, the phonon conductivity of fully filled $Ba(CoSb_3)_4$ was calculated and is also shown in Fig. 7. It is surprising that the predicted k_p of $Ba(CoSb_3)_4$ reaches 10 W m^{-1} K^{-1}, which is even higher than that of pure $CoSb_3$. This is not expected according to the traditional "rattler" idea that the filler's random "rattling" movement strongly scatters the phonons and results in a much lower phonon conductivity. Using the above force field but replacing the Ba atom and its potentials with other fillers (e.g. Ce) and their corresponding potentials, a similar

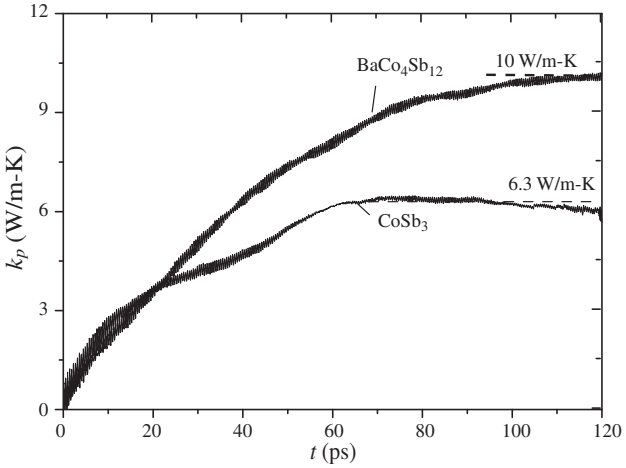

Fig. 7. Evolvement of predicted variation of the phonon conductivity of $CoSb_3$ and $Ba(CoSb_3)_4$. In the MD simulation, the modified force field of Feldman and Singh [14] was used for the host, and the Sb–Ba potential was fitted with the energy surface.

increase in the MD-predicted thermal conductivity was found. To find out the reason for this increase in phonon conductivity, we calculated the elastic properties of $Ba(CoSb_3)_4$ using the above force field. After the Ba insertion, the bulk modulus E_p increases from 99.2 to 116.8 GPa and c_{11} increases from 203 to 235 GPa. These changes suggest that the creation of a strong Ba–Sb bond makes the lattice more rigid. According to the Slack relation [31,32], $k_p \propto T_D^3 \propto E_p^{3/2}$, the change in elastic properties may thus result in 25% increase in the phonon conductivity. At the same time, the insertion of Ba atoms adds parallel paths for phonon transport, i.e. some phonons may pass through Ba–Sb bonds rather than propagate around the cage.

According to Fig. 5, we believe that the phonon conductivity of the fully filled $Ba(CoSb_3)_4$ skutterudite should be

Table 3
Interatomic potentials for $CoSb_3$ and the rattlers. Here r and θ are interatomic separation distance and bond angle. The parameters of the potentials are derived from ab initio calculations and RFT.

Interaction	Potential model	Parameters					
		$CoSb_3$			$Ba(CoSb_3)_4$		
		$\varphi_{\circ,1}$ (eV)	a_1 (Å^{-1})	$r_{\circ,1}$ (Å)	$\varphi_{\circ,2}$ (eV)	a_2 (Å^{-1})	$r_{\circ,2}$ (Å)
Pair							
Co–Sb		1.289	1.175	2.554	1.135	1.305	2.592
Co–Co		0.273	0.657	4.569	0.025	0.528	4.636
Sb–Sb (short bond)		2.24	1.039	2.888	0.863	1.20	2.993
Sb–Sb (long bond)	$\varphi_\circ\{[1-\exp(-a(r-r_\circ))]^2-1\}$	1.38	1.10	3.025	0.829	1.16	3.004
Sb–Sb (inter-rectangles)		0.702	0.864	3.473	0.657	0.921	3.474
Sb–Sb (inter-rectangles)		0.527	0.8	3.746	0.921	0.717	3.847
Co–Sb (second neighbor)		0.158	0.676	4.44	0.022	0.751	4.538
Co–Sb (third neighbor)		0.196	0.665	4.51			
Sb–Sb (Intra-rectangle)		0.573	0.65	4.182	0.742	0.606	4.239
Filler–host							
Ba–Sb					0.595	1.147	3.48
Angular							
Co–Sb–Sb (1)	$\frac{1}{2}\varphi_\theta(\cos\theta-\cos\theta_\circ)^2$	$\varphi_\theta = 0.91$ eV, $\theta_\circ = 109.2^\circ$					
Co–Sb–Sb (2)		$\varphi_\theta = 0.91$ eV, $\theta_\circ = 107.6^\circ$					

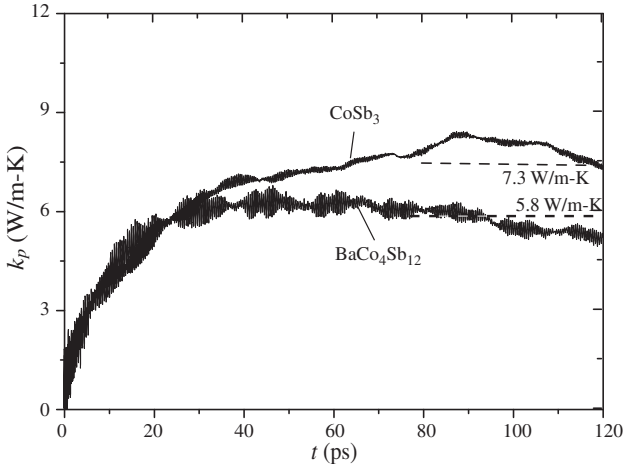

Fig. 8. Predicted variation of the phonon conductivity of $CoSb_3$ and $Ba(CoSb_3)_4$ with respect to the correlation time. In the MD simulation, the force fields developed on the basis of DFT and RFT are used.

lower than that for the empty structure, but according to the calculations above, this decrease seems to be due to the bond change resulting from the presence of Ba atoms. To confirm this further, we replaced the force fields for the host with those developed in the preceding sections on the basis of DFT and RFT (shown in Table 3) in the MD simulation. The new force fields produce $E_p = 99$ GPa and $\gamma_G = 0.96$ for $CoSb_3$, and $E_p = 78$ GPa and $\gamma_G = 1.06$ for $Ba(CoSb_3)_4$. Fig. 8 shows the predicted evolvement with these new potentials, at $T = 300$ K. These results support the suggestion that the filler "softens" the host bonds and suppresses the phonon transport.

6. Partial filling

As discussed in previous sections, the filler is strongly coupled with the host and the role of the filler in reducing the phonon conductivity is more likely to change the surrounding bonds instead of being a "rattler". It is reasonable to treat the fully filled skutterudite as a new compound which has a lower phonon conductivity. Therefore, the partially filled skutterudites can be thought of as solid solutions of completely filled and unfilled components, e.g. the partially filled $Ba_x(CoSb_3)_4$ can be considered as solid solutions of $Ba(CoSb_3)_4$ and $\square(CoSb_3)_4$. Thus, the pre-eminent mass fluctuation scattering is between Ba and □. Similar ideas for $Ce_yFe_xCo_{4-x}Sb_{12}$ have been proposed by Meisner et al. [3]. In this model, the thermal conductivity is reduced due to the less long-range order. The filler introduces extra mass centers and alters the bond structure.

We compared the experimental phonon conductivity [19] of $Ba_x(CoSb_3)_4$ with that predicted using the point defect scattering theory [33,34,3]. For high defect concentration, the phonon conductivity limited by the point defects scattering $k_{p,d}$ can be given by Meisner et al. [3]

$$k_{p,d} = k_B/[4\pi u_{p,g,A}(a_1 CT)^{1/2}], \tag{4}$$

where CT is the coefficient of the frequency-dependent relaxation time for interphonon scattering (C is a constant and T is temperature) and $u_{p,g,A}$ is the average phonon group velocity. The relaxation time for interphonon scattering can be estimated from the room-temperature thermal conductivity of empty $CoSb_3$ crystal $k_{p,CoSb_3} = 8$ W m^{-1} K^{-1} [3], i.e.

$$CT = k_B^2 T_D/(2\pi^2 u_{p,g,A}\hbar k_{p,CoSb_3}) = \frac{(6n)^{1/3}k_B}{2\pi^{4/3}k_{p,CoSb_3}}, \tag{5}$$

where n is the atomic number density. When only acoustic modes are considered, this yields $CT = 4.69 \times 10^{-16}$ s. The parameter a_1 is the coefficient for the Rayleigh-type point defect scattering rate, which is given by $a_1 = V_c a_s/(4\pi u_{p,g,A}^3)$. Here, V_c is the unit cell volume and a_s is the scattering parameter. For impurity atoms on a single atom site, $a_s = \sum f_i(1 - M_i/\langle M\rangle)^2$, where $\langle M\rangle = \sum f_i M_i$, f_i is the fractional concentration of impurity i, and M_i is its mass. The scattering parameter for a compound $Re_uM_vX_w$, denoted as $a_s(Re_uM_vX_w)$, is given by [35,3].

$$\begin{aligned} a_s(Re_uM_vX_w) = {} & \frac{u}{u+v+w}\left(\frac{M_{Re}}{M_m}\right)^2 a_s(Re) \\ & + \frac{v}{u+v+w}\left(\frac{M_M}{M_m}\right)^2 a_s(M) \\ & + \frac{w}{u+v+w}\left(\frac{M_X}{M_m}\right)^2 a_s(X), \end{aligned} \tag{6}$$

where $M_m = (u\ M_{Re} + v\ M_M + w\ M_X)/(u+v+w)$. For a solid solution of $[Ba(CoSb_3)_4]_x\ [\square(CoSb_3)_4]_{1-x}$, Re = (Ba, □)), M = Co and X = Sb. Therefore, $a_s(Re_uM_v\ X_w) = 0.095x(1-x)$. According to Eq. (4) and using [30] $u_{p,g,A} = 2934$ m s^{-1}, the thermal resistivity due to the point defects scattering is $k_{p,d}^{-1} = 0.62[x(1-x)]^{1/2}$ m-K W^{-1}. According to the Matthiessen rule [24], the overall phonon conductivity k_p(solution) of the solution $[Ba(CoSb_3)_4]_x\ [\square(CoSb_3)_4]_{1-x}$ is given by

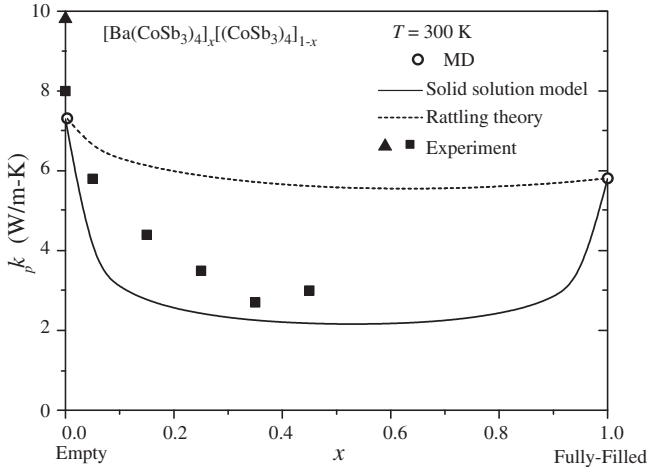

Fig. 9. Variation of predicted (using the solid solution and rattling model) phonon conductivity of $Ba_x(CoSb_3)_4$ (at $T = 300$ K), with respect to the filling fraction. The experimental results of Chen et al. [19] are also shown, as well as the MD/G–K results for $x = 0$ and $x = 1$.

$$k_p^{-1}(\text{solution}) = x k_{p,\text{Ba(CoSb}_3)_4}^{-1} + (1-x) k_{p,\text{CoSb}_3}^{-1} + k_{p,\text{d}}^{-1}. \quad (7)$$

Here there is no artificial parameter to be fitted with experimental thermal conductivity data. The variations in the predicted overall phonon conductivity k_p(solution) of $Ba_x(CoSb_3)_4$ with respect to the filling fraction (at $T = 300$ K) are shown in Fig. 9, along with the experimental results [19]. In these calculations, both $k_{p,\text{Ba(CoSb}_3)_4}$ and k_{p,CoSb_3} values are from the MD simulations. For comparison, the predictions of the rattling theory including point defects are also shown in Fig. 9. In the rattling theory, the phonon mean free path is limited by the average distance between rattlers as well as Umklapp scattering [36]. As pointed out by Nolas et al. [2], point defects might also play a role in reducing the thermal conductivity and the mass fluctuation scattering is between the entire filled structure and the empty one. Therefore, the variation of thermal conductivity with respect to x predicted by the model, considering both rattlers and point defects, nearly has the form $k_p(x) = k_p(0)/\{1 + b\,x^{1/3} + c(x)[x(1-x)]^{1/2}\}$. Here b is a constant for rattler scattering and is determined from $k_{p,\text{Ba(CoSb}_3)_4}$, and k_{p,CoSb_3}; $c(x)$ is the coefficient for point defect scattering with concentration x and is found using the full Alebes model [37] and parameters given in Ref. [2]. Fig. 9 shows that, even with the inclusion of the point defects, the rattling theory still noticeably underpredicts the scattering. On the other hand, the overall agreement between the calculated values from the solid solution model and the experimental results is fairly good. Note that the solution model overestimated the resistivity due to the point defects for $0.1 < x < 0.25$. There are several possible reasons for this deviation. First, Eq. (4) is for high defect concentrations, and it may overestimate the scattering rate at low defect concentrations. Secondly, our model assumes a homogeneous impurity distribution, where in real samples there are possibly phase segregations. Using an experimental thermal conductivity value ($8\ \text{W m}^{-1}\ \text{K}^{-1}$) rather than our MD predicted result ($7.3\ \text{W m}^{-1}\ \text{K}^{-1}$) for pure $CoSb_3$ also improves the match with the experimental curve. Fig. 9 shows that a significant reduction in thermal conductivity may occur in the alloy. Fig. 9 also shows that $k_{p,\text{solution}}$ is not very sensitive to the filling fraction x when $0.2 < x < 0.8$, which is mainly due to the dominance of defect scattering and the low $k_{p,\text{Ba(CoSb}_3)_4}$. Eq. (7) shows that the minimum value does not occur exactly at $x = 0.5$ but depends on $k_{p,\text{Ba(CoSb}_3)_4}$ and k_{p,CoSb_3}. In the solid solutions, the two distinct components have similar lattice structures, so the local order is retained (unit-cell level). This is different from glass (amorphous phase). Thus, reference to the glass behavior indicates the dominance of solution (alloy) scattering and the lack of long-range phonon transport. This solution model can also explain why the phonon conductivities of the filled skutterudites are independent of temperature at high temperatures and have lower peaks at low temperatures, since these are typical behaviors of solid solutions.

7. Summary and conclusion

In this work, both lattice vibrations and phonon transport in the empty $CoSb_3$ and filled $Ba(CoSb_3)_4$ skutterudites were investigated by performing first-principles calculations and MD simulations.

The filler–host coupling in filled $CoSb_3$ is found to be strong and its anharmonicity is minor. This differs from the traditional thought that fillers act as randomly moving "rattlers" that have weak bonds with the host. The lattice structures of both empty $CoSb_3$ and fully filled $Ba(CoSb_3)_4$ are relaxed using DFT calculations. The comparison of the two relaxed structures shows that the insertion of Ba changes the lattice constants and almost all the bond lengths. The interatomic force constants for the two relaxed structures are also calculated using DFT and RFT. The results shows that the interatomic force constant, except for Sb–Co bonds, is significantly affected by the presence of the Ba filler.

The MD simulations also shows that, without changing the interatomic interactions for the host, the addition of filler cannot reduce the phonon conductivity for filled skutterudites. The decrease in the phonon conductivity in the fully filled skutterudites seems more likely due to the weaker bonds and lattice distortion resulting from the presence of the filler.

The results for the partially filled $Ba_x(CoSb_3)_4$ skutterudites may be better understood if they are considered as the solid solutions of the empty $CoSb_3$ and the fully filled $Ba(CoSb_3)_4$. The predictions using the point defect scattering theory show a good agreement with the experimental results. This indicates the importance of alloying in reducing the phonon conductivity of skutterudites.

Acknowledgements

This work was supported by the US DOE (Department of Energy), Office of Basic Energy Sciences under Grant DE-FG02-00ER45851. The authors are thankful for the financial support of the DOE (Basic Energy Sciences) through the UM Center for Solar and Thermal Energy Conversion. The authors would like to thank Ctirad Uher for his many insightful comments.

References

[1] Uher C. Semicond Semimet 2001;69:139.
[2] Nolas GS, Cohn JL, Slack GA. Phys Rev B 1998;58:164.
[3] Meisner GP, Morelli DT, Hu S, Yang J, Uher C. Phys Rev Lett 1998;80:3351.
[4] Sales B. MRS Bull 1998;23:15.
[5] Keppens V, Mandrus D, Sales BC, Chakoumakos BC, Dai P, Coldea R, et al. Nature 1998;395:876.
[6] Uher C, Chen B, Hu S, Morelli DT, Meisner GP. MRS Sym Proc 1997;478:315.
[7] Morelli DT, Meisner GP, Chen B, Hu S, Uher C. Phys Rev B 1997;56:7376.
[8] Gonze X, Beuken JM, Caracas R, Detraux F, Fuchs M, Rignanese GM, et al. Comput Mater Sci 2002;25:478.

[9] Perdew JP, Burke K, Ernzerhof M. Phys Rev Lett 1996;77:3865.
[10] Shi X, Zhang W, Chen LD, Yang2 J. Phys Rev Lett 2005;95:185503.
[11] Ghosez P, Veithen M. J Phys: Condens Matter 2007;19:096002.
[12] Schmidt T, Kliche G, Lutz HD. Acta Crystallogr Sec C: Cryst Struct Commun 1987;43:1678.
[13] Mahan GD. Solid State Phys 1997;51:82.
[14] Feldman JL, Singh DJ. Phys Rev B 1996;53:6273.
[15] Kajitani T, Ono Y, Miyazaki Y, Sluiter M, Chen L, Goto T et al. In: 22nd International conference on thermoelectrics; 2003. p. 81.
[16] Feldman JL, Singh DJ, Mazin II, Mandrus D, Sales BC. Phys Rev B 2000;61:R9209.
[17] Koza MM, Johnson MR, Viennois R, Mutka H, Girard L, Ravot D. Nature Mater 2008;7:805.
[18] Hasegawa T, Takasu Y, Ogita N, Udagawa M. J Phys Soc Jpn 2008;77(Suppl. A):24.
[19] Chen LD, Kawahara T, Tang XF, Goto T, Hirai T, Dyck JS, et al. J Appl Phys 2001;90:1864.
[20] Giannozzi P, Gironcoli S, Pavone P, Baroni S. Phys Rev B 1991;43:7231.
[21] Braun DJ, Jeitschko W. J Solid State Chem 1980;32:357.
[22] Feldman JL, Dai P, Enck T, Sales BC, Mandrus D, Singh DJ. Phys Rev B 2006;73:014306.
[23] Tsutsui S, Kobayashi H, Sutter J, Uchiyama H, Baron A, Yoda Y. J Phys Soc Jpn 2008;77(Suppl. A):257.
[24] Kaviany M. Heat Transfer Physics. Cambridge University Press; 2008.
[25] McGaughey AJH, Kaviany M. Int J Heat Mass Trans 2004;47:1799.
[26] Huang BL, McGaughey AJH, Kaviany M. Int J Heat Mass Trans 2007;50:393.
[27] Lutz HD, Kliche G. Phys Status Solidi B 1982;112:549.
[28] Gonze X. Phys Rev B 1997;55:10337.
[29] Gonze X. Phys Rev B 1997;55:10355.
[30] Caillat T, Borshchevsky A, Fleurial J-P. J Appl Phys 1996;80:4442.
[31] Slack GA. Solid State Phys 1979;34.
[32] Huang BL, Kaviany M. J Appl Phys 2006;100:123507.
[33] Klemens PG. Phys Rev 1960;119:507.
[34] Callaway J, von Baeyer HC. Phys Rev 1960;120:1149.
[35] Slack GA. Phys Rev 1962;126:427.
[36] Sales BC, Chakoumakos BC, Mandrus D. Phys Rev B 2000;61:2475.
[37] Abeles B. Phys Rev 1963;131:1906.